Cellulose

Impact of hemicelluloses and crystal size on X-ray scattering from atomistic models of cellulose microfibrils

Supplementary information

Aleksi Zitting[1], Antti Paajanen[2], Paavo A. Penttilä[1]

[1] Department of Bioproducts and Biosystems, Aalto University, Espoo, Finland
[2] VTT Technical Research Centre of Finland Ltd, Espoo, Finland

Corresponding author email: paavo.penttila@aalto.fi

1 Analysis of molecular trajectories

1.1 Lattice spacings

The molecular trajectories were coarse-grained from atomistic to sugar unit resolution by replacing each glucose unit with a single point particle at the center of mass of its pyranose ring. The vectors adjoining the glucose units and their nearest neighbors were used to calculate local estimates for the unit cell vectors:

$$\begin{aligned}
\mathbf{a}^{+} &= 2\left(\mathbf{v}_{111} + \mathbf{v}_{11\bar{1}} + \mathbf{v}_{1\bar{1}1} + \mathbf{v}_{1\bar{1}\bar{1}}\right) \\
\mathbf{a}^{-} &= -2\left(\mathbf{v}_{\bar{1}11} + \mathbf{v}_{\bar{1}1\bar{1}} + \mathbf{v}_{\bar{1}\bar{1}1} + \mathbf{v}_{\bar{1}\bar{1}\bar{1}}\right) \\
\mathbf{b}^{+} &= \mathbf{v}_{010} \\
\mathbf{b}^{-} &= -\mathbf{v}_{0\bar{1}0} \\
\mathbf{c}^{+} &= 2\mathbf{v}_{001} \\
\mathbf{c}^{-} &= -2\mathbf{v}_{00\bar{1}}
\end{aligned}$$

where $\mathbf{v}_{ijk}$ is the vector from a glucose unit to its nearest neighbor in the direction ijk (see Figure S1) and the superscripts $^{+}$ and $^{-}$ refer to estimates in the positive and negative direction of the unit cell vector.

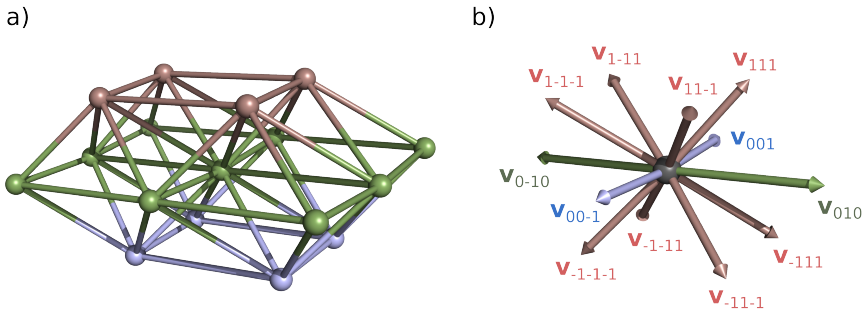

Fig. S1 (a) Coarse-grained representation of a glucose unit and its nearest neighbors within a cellulose crystal. The glucose units are shown as spheres and nearest neighbors are indicated by connecting lines. (b) The vectors from a glucose unit to its neighbors were used to approximate the unit cell vectors. Here, the subscripts do not refer to crystallographic directions.

To estimate the interplanar distances, the crystal lattice was assumed to remain monoclinic. The distances are then given by the relation:

$$d_{hkl} = \left(\frac{\left(\frac{h}{a}\right)^2 + \left(\frac{k}{b}\right)^2 + \left(\frac{l\sin\gamma}{c}\right)^2 - \frac{2hk\cos\gamma}{ab}}{\sin\gamma^2} \right)^{-\frac{1}{2}}$$

where a, b and c are the magnitudes of the unit cell vectors **a**, **b** and **c**, respectively, and γ is the angle between **a** and **b**. In the simulations, the crystal lattice does not remain strictly monoclinic, but the error introduced by this is assumed to be small. The use of nearest neighbor vectors to approximate the unit cell vectors also introduces a small error. For a perfect cellulose I_β crystal, the relative errors are $\Delta a/a = 10^{-3}$, $\Delta b/b = 10^{-4}$, $\Delta c/c = 10^{-3}$ and $\Delta\gamma/\gamma = 2 \cdot 10^{-4}$.

The local lattice spacing estimates were averaged over the glucose units of each chain, over the chains of each fibril and over time to obtain the reported values. In addition, separate analyses were carried out for the spacings of (i) surface chains and (ii) core chains (see Figure S2). In case (i) the analysis was restricted to nearest neighbor vectors between surface and surface-bound chains, and in case (ii) to those between core chains. Since the calculation of d_{200} requires knowledge of both the **a** and **b** unit cell vectors, it was not obtained for core chains missing a nearest neighbor in the [010] or [0$\bar{1}$0] direction.

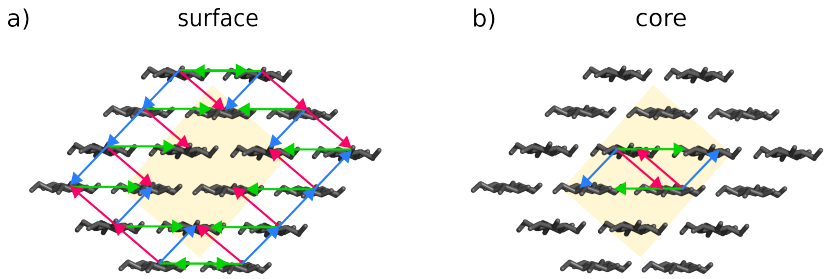

Fig. S2 Lattice spacings were estimated separately for (a) surface and (b) core chains. For each glucose unit, the blue and red arrows indicate the pair of chains that was used to estimate the unit cell vector **a**, and the green arrow indicates the chain that was used to estimate the unit cell vector **b**. For surface chains, the first layer of sub-surface chains was included in the analysis.

1.2 Fibril width

Fibril width was estimated based on distances between the outermost chain pairs in directions perpendicular to the (200), (110) and (1$\bar{1}$0) crystallographic planes (Figure S3). Averaging was carried out over the glucose units of each chain pair, over the chain pairs and over time.

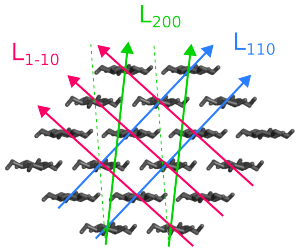

Fig. S3 Fibril width was estimated in different crystallographic directions based on the distance between the outermost chain pairs in each direction (shown by the solid line arrows). It should be noted that the width estimate in the [200] direction (L_{200}) is not strictly the same as the interplanar distance. Moreover, it depends on the number of chain layers, as shown by the difference between the solid and dashed green lines (dashed line parallel to the unit cell vector **a**).

1.3 Radial electron density distribution

The radial electron density distribution, $\rho(r)$, was calculated with respect to the principal axis of the fibril and with the electrons counted at the locations of atomic nuclei. The used spatial resolution was 1 pm and time averaging was applied over the trajectory. A two-step function of the form

$$\rho_{\mathrm{cs}}(r) = \begin{cases} \rho_{\mathrm{core}} & , r \in [0,\ R] \\ \rho_{\mathrm{shell}} & , r \in\ ]R,\ R+t] \\ 0 & , r \in\ ]R+t,\ \infty] \end{cases}$$

was fitted against the radial distribution to get a core-shell cylinder approximation of the electron density (Figure 2b of the main article). The uncertainties of the core radius (ΔR) and shell thickness (Δt) were estimated as follows. First, an asymmetric peak was formed at the location of each step (i.e. at $r = R$ and $r = R+t$) by subtracting the density at radial distances below the step location from the density at the step:

$$\rho_{\mathrm{p1}}(r) = \begin{cases} 2\rho(R) - \rho(r) & , r \in [0,\ R] \\ \rho(r) & , r \in\ ]R,\ \infty] \end{cases}$$

$$\rho_{\mathrm{p2}}(r) = \begin{cases} 2\rho(R+t) - \rho(r) & , r \in [0,\ R+t] \\ \rho(r) & , r \in\ ]R+t,\ \infty] \end{cases}$$

A Gaussian function was then fitted against each peak and the integral breadth of the Gaussian was used as an estimate for the uncertainty of the step location.

2 Scattering results

2.1 Straight fibrils

2.1.1 Effects of hemicelluloses

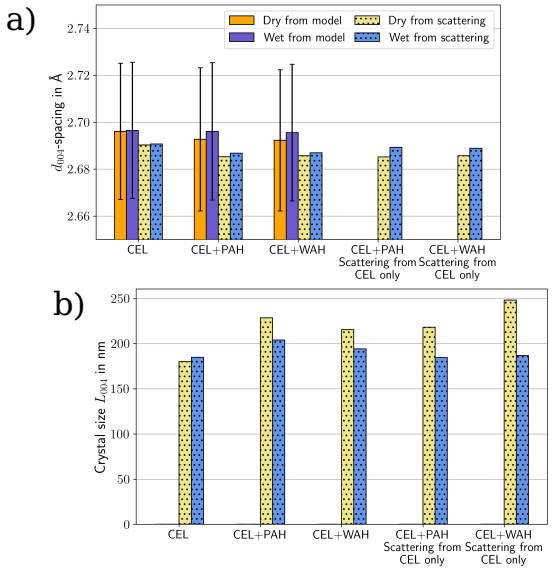

Fig. S4 (a) Lattice spacing d_{004} and (b) crystal size L_{004} for straight fibrils with different hemicellulose coatings

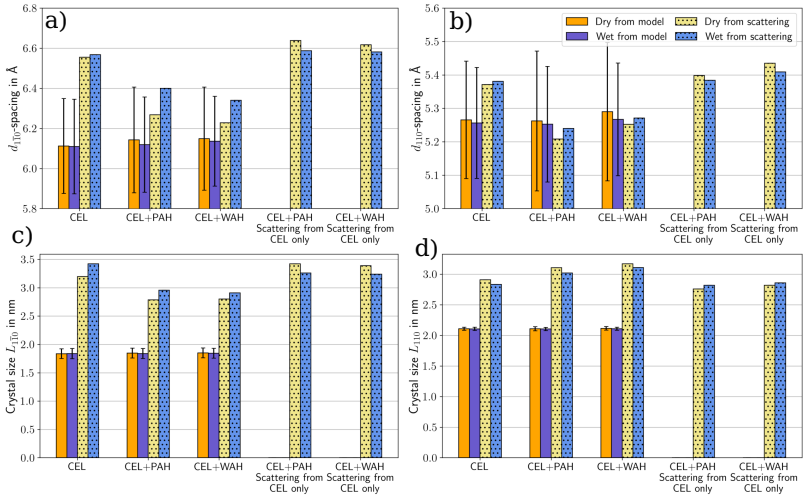

Fig. S5 (a, b) Lattice spacings $d_{1\bar{1}0}$, d_{110} and (c, d) crystal size $L_{1\bar{1}0}$, L_{110} for straight fibrils with different hemicellulose coatings

2.1.2 Effects of crystal size

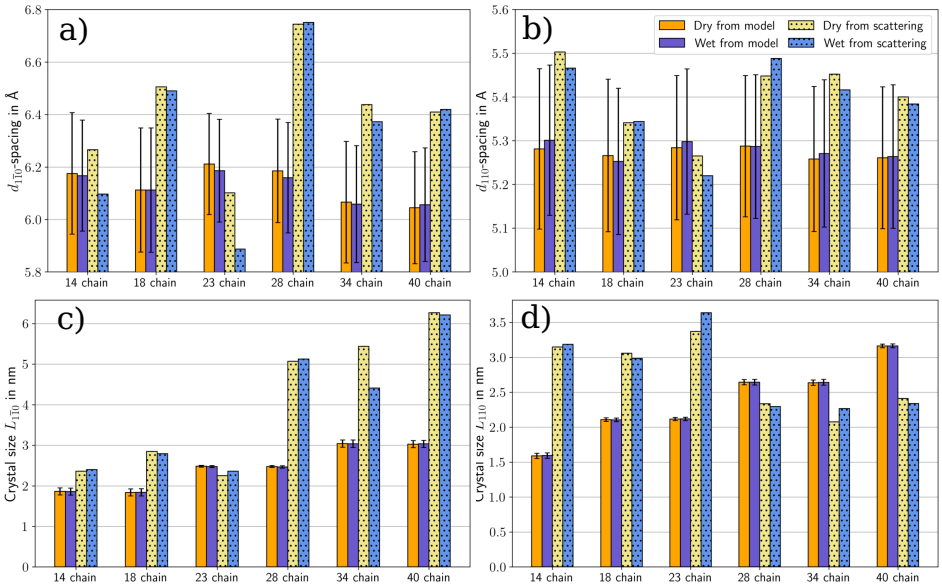

Fig. S6 (a, b) Lattice spacings $d_{1\bar{1}0}$, d_{110} and (c, d) crystal size $L_{1\bar{1}0}$, L_{110} for straight fibrils with different crystal sizes

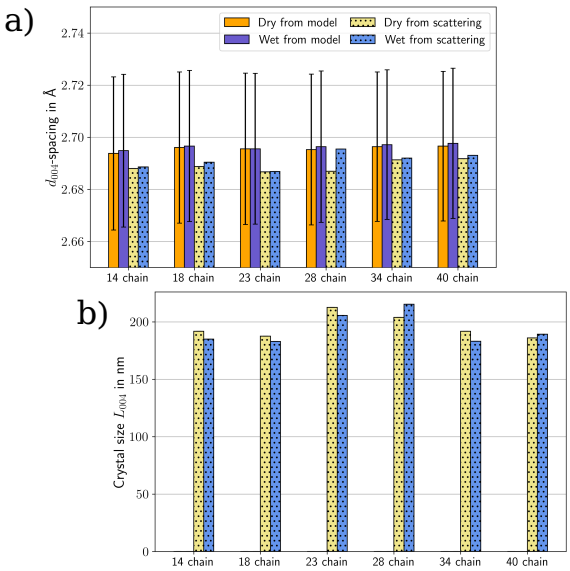

Fig. S7 (a) Lattice spacing d_{004} and (b) crystal size L_{004} for straight fibrils with different crystal sizes

2.2 Twisting fibrils

2.2.1 Effects of hemicelluloses

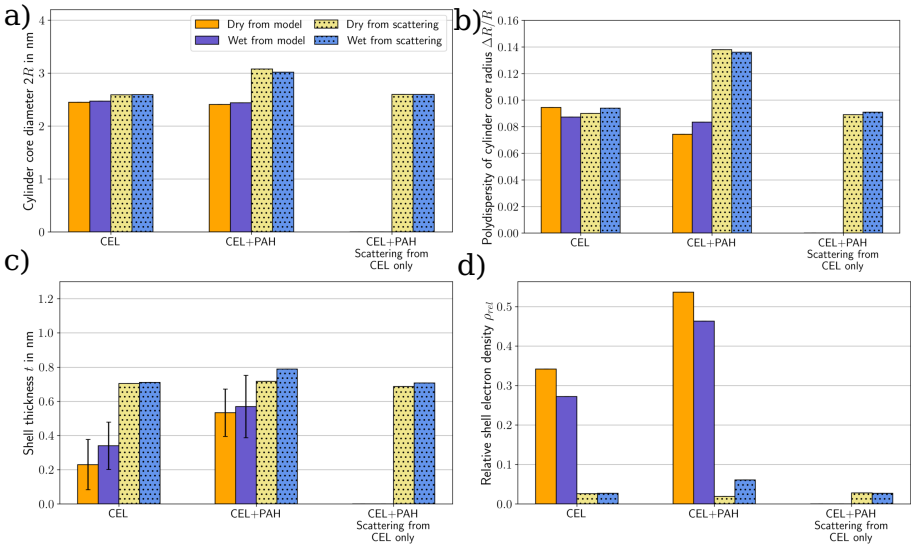

Fig. S8 SAXS fitting parameters for twisting fibrils with different hemicellulose coatings: (a) Cylinder core diameter $2R$, (b) Polydispersity of cylinder core radius $\Delta R/R$, (c) Shell thickness t, (d) Relative shell electron density ρ_{rel}

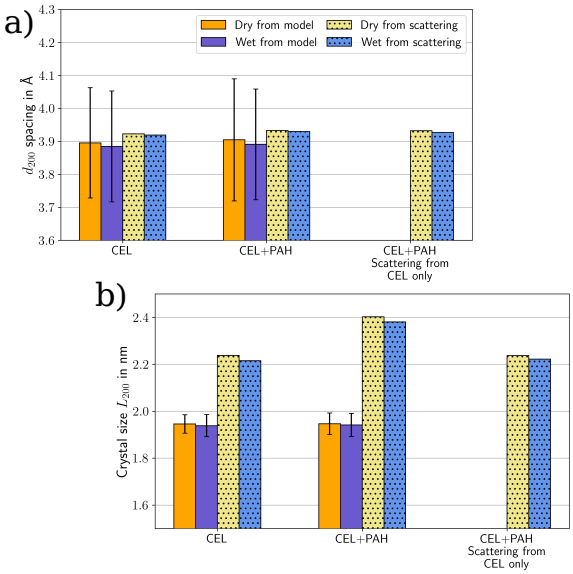

Fig. S9 (a) Lattice spacing d_{200} and (b) crystal size L_{200} for twisting fibrils with different hemicellulose coatings

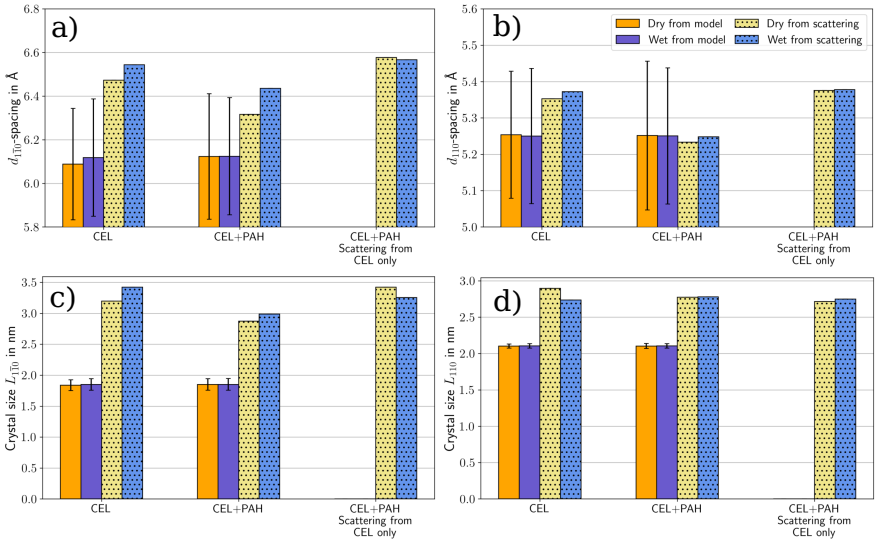

Fig. S10 (a, b) Lattice spacings $d_{1\bar{1}0}$, d_{110} and (c, d) crystal size $L_{1\bar{1}0}$, L_{110} for twisting fibril with different hemicellulose coatings

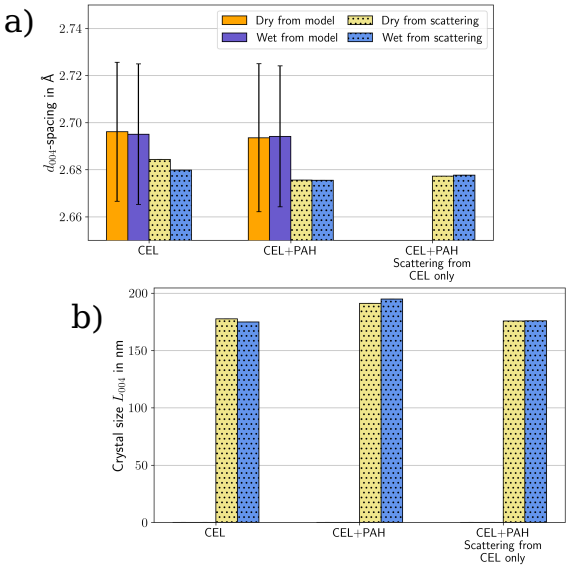

Fig. S11 (a) Lattice spacing d_{004} and (b) crystal size L_{004} for twisting fibrils with different hemicellulose coatings

2.2.2 Effects of crystal size

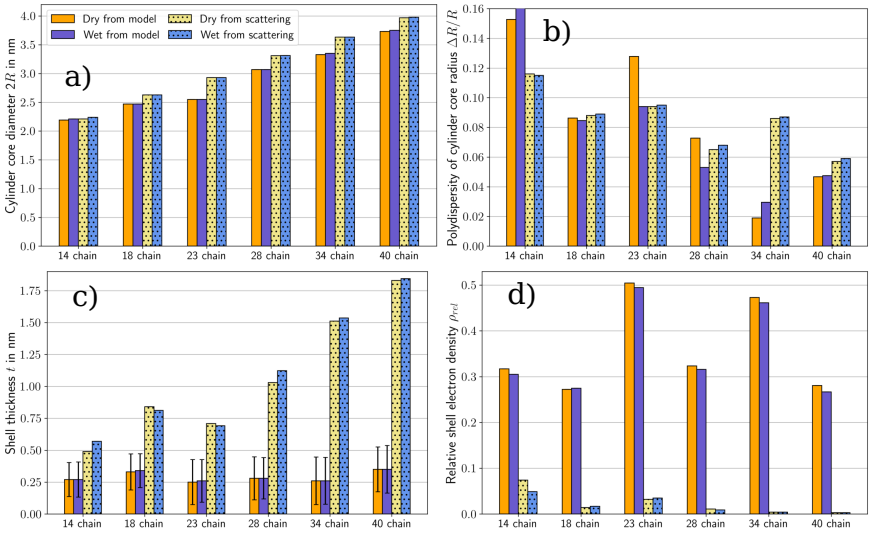

Fig. S12 SAXS fitting parameters for twisting fibrils with different crystal sizes: (a) Cylinder core diameter $2R$, (b) Polydispersity of cylinder core radius $\Delta R/R$, (c) Shell thickness t, (d) Relative shell electron density ρ_{rel}

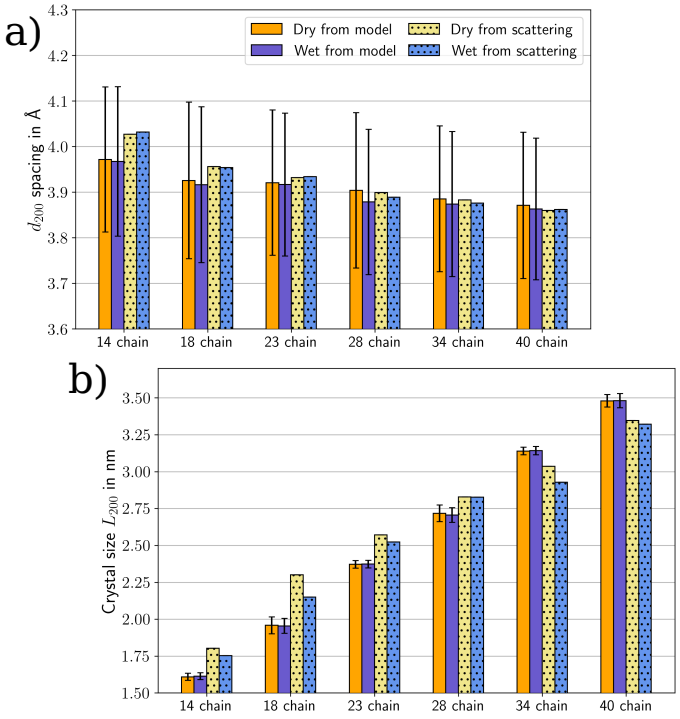

Fig. S13 (a) Lattice spacing d_{200} and (b) crystal size L_{200} for twisting fibrils with different crystal sizes

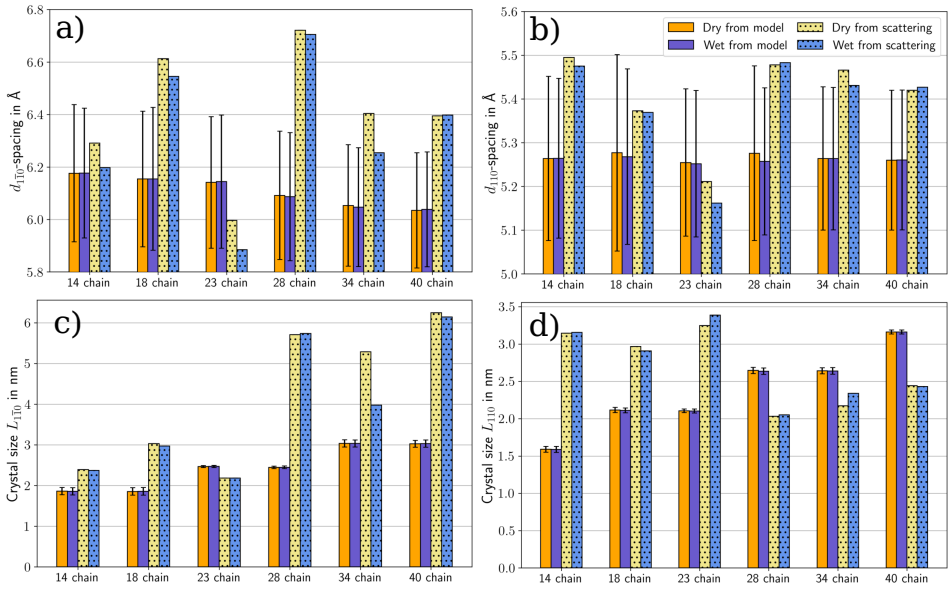

Fig. S14 (a, b) Lattice spacings $d_{1\bar{1}0}$, d_{110} and (c, d) crystal size $L_{1\bar{1}0}$, L_{110} for twisting fibrils with different crystal sizes

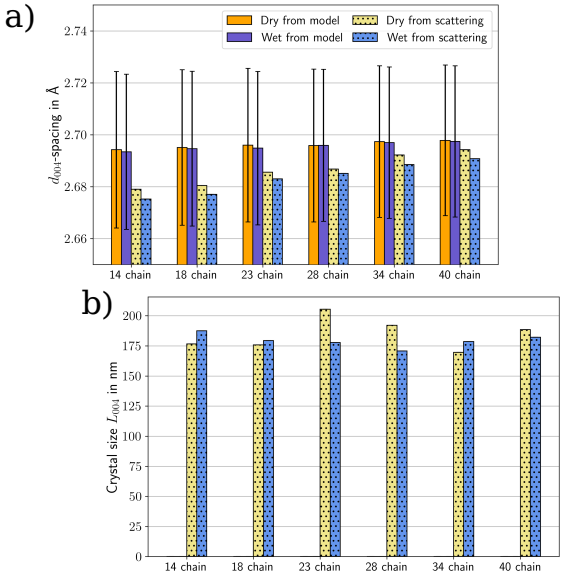

Fig. S15 (a) Lattice spacing d_{004} and (b) crystal size L_{004} for twisting fibrils with different crystal sizes